

Theory of ac Josephson effect and noise in superconducting constrictions

Dmitri V. Averin

Department of Physics and Astronomy, SUNY at Stony Brook, Stony Brook, New York, 11794, USA

I. INTRODUCTION

In contrast to point contacts between normal metals, the superconducting point contacts have very non-trivial transport properties even under the simplest bias conditions of fixed dc bias voltage V across the contact. The origin of this complexity is the oscillating Josephson current induced in the point contact by non-vanishing bias voltage which makes electron motion through the contact inelastic. From the microscopic point of view, this type of inelastic electron dynamics can be understood in terms of cycles of Andreev reflections at the two interfaces between the contact and superconducting electrodes [1]. Electron emerging from, say, the left electrode with energy ε relative to the Fermi level of this electrode is accelerated by the applied voltage V and reaches the right electrode having the energy $\varepsilon + eV$. It is then Andreev-reflected back as a hole which is again *accelerated* when crossing the contact backward. After being Andreev-reflected from the left electrode this hole produces an electron with the energy $\varepsilon + 2eV$ (Fig. 1a). Because of this process of multiple Andreev reflections (MAR) electron with energy ε incident on the contact can absorb or emit some number n of quanta $2eV$ of the Josephson oscillations and emerge from the contact area with the energy $\varepsilon + 2neV$.

Phenomenologically, the cycles of MAR manifest themselves in the so-called “subharmonic gap structure” (SGS) in the current-voltage characteristics of the superconducting contacts: current singularities at voltages $V_n = 2\Delta/en$, $n = 2, 3, \dots$, where Δ is the superconducting energy gap of the contact electrodes. Since the cycle of two Andreev reflections requires that both electron and hole traverse the contact, the probability of this process is proportional to D^2 in contacts with small transparency D . This means that in junctions with the low-transparent barriers, the MAR current is much smaller than the regular quasiparticle current or current of Cooper pairs which both scale as D with junction transparency. There is, however, a very large variety of high-transparency Josephson junctions, where multiple Andreev reflections and associated subharmonic gap structure are important. Possible implementations of the high-transparency junctions include tunnel junctions with high critical current density [2], semiconductor/superconductor heterostructures [3,4], controllable break junctions [5–7], disordered superconductor/semiconductor junctions [8,9], short metallic SNS junctions [10].

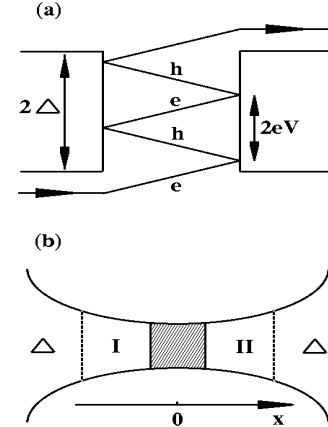


FIG. 1. (a) Schematic energy diagram of the multiple Andreev reflections process in a ballistic constriction between two superconductors with energy gap Δ . Both electrons and holes are accelerated by the applied bias voltage V and gain energy eV crossing the constriction. (b) Geometry of the constriction. The shaded area corresponds to the scattering region. The pair potential $\Delta(x)$ can be neglected in regions I and II.

The subharmonic gap structure was extensively studied in experiments done in the 60’s [11–15], and was interpreted in terms of the multi-particle tunneling [18]. However, the theory [18] of multi-particle tunneling is valid only in the limit of low junction transparency, $D \rightarrow 0$, and can not account quantitatively for all features of the SGS. A more detailed understanding of the SGS was developed later [1,19–21] based on the idea of MAR. Nevertheless, quantitative dependence of the SGS on the contact transparency D was still not fully understood at that time. During the last few years, considerable progress has been made in quantitative description of MAR in short constrictions (shorter than the coherence length ξ of the superconducting electrodes of the constriction) with arbitrary transparency [22–26]. The aim of this Chapter is to review these recent developments. Section 2 presents the scattering approach to MAR in the multi-mode constrictions, in particular, in short disordered SNS junctions. In Section 3 we discuss the Green’s function approach to description of MAR which is needed to account for the effects of non-trivial microscopic structure of the constriction electrodes. In Section 4 the noise properties of the ballistic constrictions are calculated starting from the results obtained in Section 3. The Conclusion summarizes the results and unsolved problems of the theory of

ac Josephson effect in high-transparency Josephson junctions.

II. MULTI-MODE CONSTRICTIONS

The main simplification brought about by the condition $d \ll \xi$, where d is the characteristic dimensions of the constriction, is the possibility of neglecting, first, all properties of the constriction besides its normal-state scattering matrix S , and second, all deviations from equilibrium in the electrodes of the constriction [27,19]. These two factors allow to avoid the self-consistent determination of both the pair potential and electrostatic potential. Electron transport through the constriction is determined then by the interplay of scattering in the constriction (described by S), acceleration of quasiparticles in the constriction by the bias voltage V , and Andreev reflection with the amplitude $a(\varepsilon)$ at the two interfaces with the superconducting electrodes in equilibrium,

$$a(\varepsilon) = \frac{1}{\Delta} \begin{cases} \varepsilon - \text{sign}(\varepsilon)(\varepsilon^2 - \Delta^2)^{1/2}, & |\varepsilon| > \Delta, \\ \varepsilon - i(\Delta^2 - \varepsilon^2)^{1/2}, & |\varepsilon| < \Delta. \end{cases} \quad (1)$$

Here ε is the quasiparticle energy relative to the Fermi level of the electrode, and Δ is the equilibrium energy gap of the electrodes.

To find the transport properties of the constriction quantitatively, we generalize [23,28] to non-vanishing bias voltages V the scattering approach for Bogolyubov-de Gennes equations [29–31] that describes dc Josephson effect at $V = 0$. In accordance with the qualitative picture of MAR discussed in the Introduction, electron with energy ε incident on the constriction generates electron and hole states at energies $\varepsilon + 2neV$ with arbitrary n . Thus, the electron and hole wavefunctions in regions I and II of the constriction (Fig. 1b) can be written as follows:

$$\begin{aligned} \text{(I)} \quad \psi_{el} &= \sum_n [(a_{2n}A_n + J\delta_{n0})e^{ikx} + B_ne^{-ikx}]e^{-i(\varepsilon+2neV)t/\hbar}, \\ \psi_h &= \sum_n [A_ne^{ikx} + a_{2n}B_ne^{-ikx}]e^{-i(\varepsilon+2neV)t/\hbar}, \end{aligned} \quad (2)$$

$$\begin{aligned} \text{(II)} \quad \psi_{el} &= \sum_n [C_ne^{ikx} + a_{2n+1}D_ne^{-ikx}]e^{-i(\varepsilon+(2n+1)eV)t/\hbar}, \\ \psi_h &= \sum_n [a_{2n+1}C_ne^{ikx} + D_ne^{-ikx}]e^{-i(\varepsilon+(2n+1)eV)t/\hbar}, \end{aligned} \quad (3)$$

where $a_n \equiv a(\varepsilon + neV)$. In these equations we took into account that the amplitudes of electron and hole wavefunctions are related by the Andreev reflection, and also neglected variations of the quasiparticle momentum k with energy assuming that the Fermi energy in the electrodes is much larger than Δ . The quasiparticle energies in regions I and II are measured relative to the Fermi level in the left and right electrode, respectively. Since the constriction is assumed to support N propagating transverse

modes, all amplitudes of the electron and hole wavefunctions have transverse mode index m not shown in eqs. (2) and (3), e.g., $A_n \equiv \{A_{n,m}\}$, $m = 1, \dots, N$. The source term J describes an electron generated in the j th transverse mode by a quasiparticle incident on the constriction from the left superconductor: $J(\varepsilon) = (1 - |a_0|^2)^{1/2} \delta_{mj}$.

The current in the constriction can be calculated in terms of the electron and hole wavefunctions in the region I or II. The contribution $i(t)$ to the current from the wavefunction (2) is:

$$i(t) = \frac{e\hbar}{m} \text{ImTr}(\psi_{el} \nabla \psi_{el}^\dagger - \psi_h \nabla \psi_h^\dagger), \quad (4)$$

where Tr is taken over the transverse modes. Equations (2) and (4) imply that the total current $I(t)$ in the constriction oscillates with the Josephson frequency $\omega_J = 2eV/\hbar$ and can be expanded in the Fourier components:

$$I(t) = \sum_k I_k e^{ik\omega_J t}.$$

Substituting eq. (2) into (4) and summing the contributions from quasiparticles incident both from the left and right superconductors at different energies ε we obtain the Fourier components I_k of the current:

$$\begin{aligned} I_k &= -\frac{e}{\pi\hbar} \int_{-\mu-eV}^{\mu} d\varepsilon \tanh\left\{\frac{\varepsilon}{2T}\right\} \text{Tr}[(JJ^\dagger \delta_{k0} + \\ &\quad a_{2k}^* J A_k^\dagger + a_{-2k} A_{-k} J^\dagger + \\ &\quad \sum_n (1 + a_{2n} a_{2(n+k)}^*) (A_n A_{n+k}^\dagger - B_n B_{n+k}^\dagger)] \Big|_{\mu \rightarrow \infty}. \end{aligned} \quad (5)$$

The amplitudes A , B , C , D of electron and hole wavefunctions (2) and (3) are related by the matrix S of scattering in the constriction. Taking into account that the scattering matrix for the holes is the time-reversal conjugate of electron scattering matrix S we can write:

$$\begin{pmatrix} B_n \\ C_n \end{pmatrix} = S \begin{pmatrix} a_{2n}A_n + J\delta_{n0} \\ a_{2n+1}D_n \end{pmatrix}, \quad (6)$$

$$\begin{pmatrix} A_n \\ D_{n-1} \end{pmatrix} = S^* \begin{pmatrix} a_{2n}B_n \\ a_{2n-1}C_{n-1} \end{pmatrix}, \quad (7)$$

The scattering matrix S is a unitary and symmetric matrix $2N \times 2N$ and can be written in terms of reflection and transmission $N \times N$ matrices r , t :

$$S_{el} = \begin{pmatrix} r & t \\ t' & r' \end{pmatrix}, \quad (8)$$

where $t' = t^T$, $r' = -(t^*)^{-1} r^\dagger t$, and $tt^\dagger + rr^\dagger = 1$.

Eliminating A_n between eq. (6) and inverse of eq. (7) we find the relation between the amplitudes B_n and D_n .

Combining this relation with the expression for D_n in terms of B_n that follows from the inverse of eq. (6) and eq. (7) we arrive at the following recurrence relation for B_n :

$$tt^\dagger \left(\frac{a_{2n+2}a_{2n+1}}{1-a_{2n+1}^2} B_{n+1} - \left(\frac{a_{2n+1}^2}{1-a_{2n+1}^2} + \frac{a_{2n}^2}{1-a_{2n-1}^2} \right) B_n + \frac{a_{2n}a_{2n-1}}{1-a_{2n-1}^2} B_{n-1} \right) - [1-a_{2n}^2] B_n = -rJ\delta_{n0}, \quad (9)$$

In a similar way we obtain the recurrence relation for the amplitudes A_n :

$$t^*t^T \left(\frac{a_{2n+1}a_{2n}}{1-a_{2n+1}^2} A_{n+1} - \left(\frac{a_{2n}^2}{1-a_{2n+1}^2} + \frac{a_{2n-1}^2}{1-a_{2n-1}^2} \right) A_n + \frac{a_{2n-1}a_{2n-2}}{1-a_{2n-1}^2} A_{n-1} + \frac{(a_1\delta_{n1} - a_0\delta_{n0})J}{1-a_1^2} \right) - [1-a_{2n}^2] A_n = -a_0J\delta_{n0}. \quad (10)$$

Since the hermitian matrix tt^\dagger can always be diagonalized by an appropriate unitary transformation U , the recurrence relation (9) implies that the structure of the amplitudes B_n as vectors in the transverse-mode space is:

$$B_n = U^\dagger f_n(D) U r J, \quad (11)$$

where $D = U t t^\dagger U^\dagger$ is the diagonal matrix of transmission probabilities D_m , $m = 1, \dots, N$. The functions $f_n(D)$ are determined by the solution of the recurrence relation (9) with the diagonalized transmission matrix tt^\dagger .

Equation (11) shows that the contribution of the amplitudes B_n to the currents (5) can be written as

$$\text{Tr}[B_n B_{n'}^\dagger] = (1 - |a_0|^2) \text{Tr}[f_n(D) f_{n'}^*(D) (1 - D)],$$

i.e., it can be represented as a sum of independent contributions from different transverse modes with the transparencies D_m . Similarly, the recurrence relation (10) and eq. (5) for the currents show that the same is true for the amplitudes A_n . Therefore, the Fourier components (5) of the total current can be written as sums of independent contributions from individual transverse modes:

$$I_k = \sum_m I_k(D_m), \quad (12)$$

where the contribution of one (spin-degenerate) mode is:

$$I_k(D) = \frac{e}{\pi\hbar} \left[eV D \delta_{k0} - \int d\epsilon \tanh\left\{ \frac{\epsilon}{2T} \right\} (1 - |a_0|^2) (a_{2k}^* A_k^* + a_{-2k} A_{-k} + \sum_n (1 + a_{2n} a_{2(n+k)}^*) (A_n A_{n+k}^* - B_n B_{n+k}^*)) \right]. \quad (13)$$

with the integral over ϵ taken in large symmetric limits. The amplitudes B_n in this equation are determined by the recurrence relation which follows directly from eq. (9):

$$D \frac{a_{2n+2}a_{2n+1}}{1-a_{2n+1}^2} B_{n+1} - [D \left(\frac{a_{2n+1}^2}{1-a_{2n+1}^2} + \frac{a_{2n}^2}{1-a_{2n-1}^2} \right) + 1 - a_{2n}^2] B_n + D \frac{a_{2n}a_{2n-1}}{1-a_{2n-1}^2} B_{n-1} = -R^{1/2} \delta_{n0}, \quad R \equiv 1 - D. \quad (14)$$

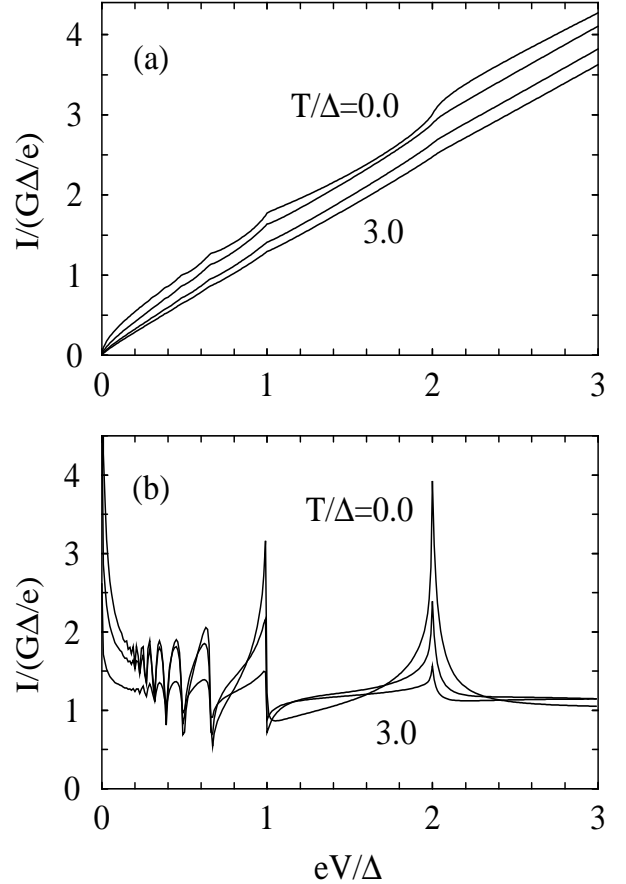


FIG. 2. (a) DC IV characteristics and (b) differential conductance dI/dV of a short disordered SNS junction at several temperatures: $T/\Delta = 0, 1, 2, 3$. (The $T = 2\Delta$ curve is omitted in (b).) The curves show the subharmonic gap singularities at $eV = 2\Delta/n$, $n = 1, 2, \dots$ associated with the multiple Andreev reflections. The differential conductance diverges as $V^{-1/2}$ at small voltages – see text.

Instead of using similar independent recurrence relation for A_n that follows from eq. (10), it is more convenient to determine these coefficients from an equivalent relation that can be obtained from a single-mode version of eqs. (6) and (7) [23]:

$$A_{n+1} - a_{2n+1}a_{2n}A_n = R^{1/2}(B_{n+1}a_{2n+2} - B_na_{2n+1}) + a_1\delta_{n0}, \quad (15)$$

The recurrence relations (14) and (15) can be solved explicitly in the case of perfect transmission, $D = 1$. In the general case of arbitrary D they provide an efficient algorithm for numerical evaluation of the current. Therefore, eqs. (12) – (15) determine completely the time-dependent current in a short constriction with arbitrary distribution of transmission probabilities. In particular, we can use these equations to calculate the current in a short disordered SNS junction with large number of transverse modes $N \gg 1$ and diffusive electron transport in the N region. The distribution of transmission probabilities is then quasicontinuous, and is characterized by the density function $\rho(D)$ (see, e.g., [32] and references therein):

$$\sum_m \dots = \int_0^1 dD \rho(D) \dots, \quad \rho(D) = \frac{\pi \hbar G}{2e^2} \frac{1}{D(1-D)^{1/2}}, \quad (16)$$

where G is the normal-state conductance of the N region. This distribution determines various transport properties of disordered mesoscopic conductors, for instance, the magnitude of the shot-noise suppression [33,34].

Figure 2 shows the results of the numerical calculations of the dc current-voltage (IV) characteristics and differential conductance of the short SNS Josephson junction obtained by averaging the single-mode contributions to the current determined from eqs. (13) – (15) over the distribution (16). We see that the IV characteristics has all qualitative features of the high-transparency Josephson junctions: subgap current singularities at $eV = 2\Delta/n$ and excess current I_{ex} at $eV \gg 2\Delta$. It is instructive to compare quantitatively these features to those in the IV characteristics of a single-mode Josephson junctions plotted in [23]. Such a comparison shows that the magnitude of the excess current in the SNS junction, as well as the overall level of current in the sub-gap region correspond approximately to a single-mode junction with large transparency $D \simeq 0.8$. At the same time, the subharmonic gap structure and the gap feature at $eV = 2\Delta$ are much more pronounced than in a single-mode junction of this transparency. The amplitude of the oscillations of the differential conductance corresponds roughly to the junction with $D \simeq 0.4$ (although this comparison is not very accurate because of the different shapes of the curves). This “discrepancy” reflects the two-peak structure of the transparency distribution (16) of the diffusive conductor: the abundance of nearly ballistic modes leads to large excess and subgap currents, while the peak at low transparencies determines the SGS features.

The main qualitative difference between the IV characteristics of the single-mode and diffusive SNS junction lies in the low-voltage ($eV \ll \Delta$) behavior of the curves. As shown below, in contrast to a single-mode junction, the IV characteristics of the SNS junction have a square-root singularity at low voltages which directly reflects the

shape of the high-transparency peak in the distribution (16). All this implies that the highly nonlinear character of the IV characteristics of the diffusive SNS junctions could serve as a direct experimental test of the transparency distribution (16) of the disordered mesoscopic conductor.

Besides providing the basis for numerical evaluation of the current, the recurrence relations (14) and (15) can be used to find the current analytically at small and large voltages. At large voltages ($eV \gg \Delta$), the probability of MAR cycles decreases rapidly with the number of Andreev reflections in them. We can then explicitly solve the recurrence relations limiting ourselves to the cycles with two Andreev reflections and find the current from eq. (13). For a single mode at $T \ll \Delta$ we get the following high-voltage asymptote of the dc current [28]:

$$I(V) = \frac{eD}{\pi \hbar} \left[eV + \frac{\Delta D}{R} \left(1 - \frac{D^2}{2\sqrt{R}(1+R)} \ln \left(\frac{1+\sqrt{R}}{1-\sqrt{R}} \right) \right) - \frac{\Delta^2}{2eV} \right]. \quad (17)$$

Averaging this result with the distribution (16) we can obtain similar asymptote for an SNS junction:

$$I(V) = G(V + \frac{\Delta}{e} (\frac{\pi^2}{4} - 1) - \frac{\Delta^2}{2eV}). \quad (18)$$

The second term in this equation represents the excess current I_{ex} and was first found in [36] by the quasiclassical Green’s function method. It can be checked that the asymptote (18) agrees well with the numerically calculated zero-temperature IV characteristic shown in Fig. 2a. The large-voltage approximation allows us also to find the asymptotes of the ac components of the current [28].

The IV characteristics of the SNS junction can also be calculated analytically at small voltages, $eV \ll \Delta$, using the understanding [23,35] that the small finite voltage V drives the Landau-Zener transitions between the Andreev-bound states of the modes with small reflection coefficients $R \ll 1$. For a single mode of this type, the nonequilibrium voltage-induced contribution to the current at $T \ll \Delta$ is [23]:

$$I(\varphi) = \frac{e\Delta}{\hbar} \begin{cases} 0, & 0 < \varphi < \pi, \\ 2 \exp\{-\pi R \Delta / eV\} \sin \varphi / 2, & \pi < \varphi < 2\pi, \end{cases} \quad (19)$$

where $\varphi = \varphi_0 + 2eVt/\hbar$ is the Josephson phase difference between the superconductors. Averaging this equation with the distribution (16) and adding the equilibrium supercurrent from [37] we obtain the dynamic current-phase relation of an SNS Josephson junction at $eV \ll \Delta$:

$$I(\varphi) = \frac{G\Delta}{e} \left(\cos(\frac{\varphi}{2}) \tanh^{-1}[\sin(\frac{\varphi}{2})] + \right.$$

$$+ \begin{cases} 0, & 0 < \varphi < \pi, \\ \pi\sqrt{eV/\Delta}\sin(\varphi/2), & \pi < \varphi < 2\pi. \end{cases} \quad (20)$$

The dc current I at small voltages is obtained by averaging eq. (20) over the phase φ :

$$I = G\sqrt{V\Delta}/e. \quad (21)$$

This square-root behavior of the current leads to the zero-bias singularity of the differential conductance of the SNS junction which can be seen in Fig. 2b. Physically, this large conductance is caused by overheating of electrons in the N region by the MAR process. Electrons with energies inside the energy gap traverse the constriction many times and as a result are accelerated to energies much larger the eV . This means that the effective voltage drop across the constriction is much larger than V , leading to increased conductance. This mechanism of conductance enhancement is qualitatively similar to the so-called “stimulation of superconductivity” [38] (which is one of the plausible explanations of the zero-bias conductance singularities [39] in long semiconductor Josephson junctions), although quantitatively the phenomena are quite different. One of the most important differences between the short and long SNS junctions is that the singularity (21) in short junctions should be suppressed by temperature simultaneously with the dc critical current, whereas in long junctions there is a temperature range where the zero-bias singularity is pronounced while the supercurrent is already negligible.

The fact that the singularity (21) is caused by electron overheating implies that it should be regularized by any mechanism of inelastic scattering. Nevertheless, in constrictions shorter than inelastic scattering length l_{in} in the normal metal, the square-root conductance singularity should be experimentally observable at low temperatures, $T \ll \Delta$, when the inelastic scattering in superconductors is also suppressed.

All of the calculations presented in this Section were based on the assumption of ideal BCS electrodes of the constriction that are characterized by the Andreev reflection amplitude (1). This assumption allows to describe dynamics of Andreev reflection with the Bogolyubov-de Gennes (BdG) equations. The most noticeable drawback of this approach is the impossibility of incorporating inelastic scattering in the electrodes which plays an important role in regularizing low-voltage singularities associated with MAR. In the next Section we show how the BdG approach can be generalized to superconductors with arbitrary microscopic structure which in general includes inelastic processes.

III. SUPERCONDUCTORS WITH GENERAL MICROSCOPIC STRUCTURE

The method that allows to discuss the inelastic effects in the superconducting electrodes of the constriction employs the quasiclassical non-equilibrium Green’s functions. For the general introduction to this technique see, e.g., [40]. In this method, position dependent density of states of the superconductors is described with the retarded and advanced Green’s function $G_{R,A}(x, \varepsilon, \varepsilon')$. Deep inside the superconducting electrodes $G_{R,A}$ reach their equilibrium position-independent form:

$$G_{R,A}^{(0)}(\varepsilon, \varepsilon') = \begin{pmatrix} g_{R,A}(\varepsilon) & f_{R,A}(\varepsilon) \\ -f_{R,A}(\varepsilon) & -g_{R,A}(\varepsilon) \end{pmatrix} \delta(\varepsilon - \varepsilon'), \quad (22)$$

where g and f are the normal and anomalous Green’s function of the superconductor which satisfy the normalization condition: $g^2 - f^2 = 1$. Retarded and advanced functions are related simply as

$$g_A(\varepsilon) = -g_R^*(\varepsilon), \quad f_A(\varepsilon) = -f_R^*(\varepsilon).$$

Space dependence of $G_{R,A}$ is governed by the equation [41,19]:

$$i\text{sign}(p_x)v_F \frac{\partial G_{R,A}}{\partial x} = [H_{R,A}, G_{R,A}], \quad (23)$$

where v_F is the Fermi velocity, $\text{sign}(p_x)$ denotes two directions of propagation in the constriction, and H is the effective matrix Hamiltonian of the superconductor. Since equation (23) should be satisfied also in equilibrium, H as a matrix commutes with $G^{(0)}$. Therefore, assuming electron-hole symmetry we can express it as

$$H_{R,A} = \Omega_{R,A} G_{R,A}^{(0)},$$

where $\Omega(\varepsilon)$ is complex quasiparticle energy. Imaginary part of Ω comes from the imaginary part of electron self-energy and is positive:

$$\text{Im}\Omega_{R,A} > 0. \quad (24)$$

In order to calculate the current through the constriction we need to find the Green’s functions inside it. Equation (23) shows that the characteristic length scale of Green’s function variation is the coherence length $\xi = \hbar v_F/\Delta$. In our model of short constriction with length d much smaller than ξ this means that from the perspective of eq. (23) all points of the constriction correspond to $x = 0$. Equation (23) determines the Green’s functions at $x = 0$ through the condition that corrections \bar{G} to the equilibrium functions (22) should decay inside the electrodes. To see how this condition translates into the matrix structure of \bar{G} we perform a “rotation” in the electron-hole space which diagonalizes $G^{(0)}$ (and hence H):

$$\tilde{G}_{R,A}(\epsilon, \epsilon') \rightarrow U_{R,A}(\epsilon) G_{R,A}(\epsilon, \epsilon') U_{R,A}^{-1}(\epsilon'), \quad (25)$$

where the rotation matrix is

$$U_{R,A} = \frac{1}{\sqrt{1 - a_{R,A}^2}} \begin{pmatrix} 1 & a_{R,A} \\ a_{R,A} & 1 \end{pmatrix}.$$

Here

$$a_R(\epsilon) = \frac{f_R(\epsilon)}{g_R(\epsilon) + 1}, \quad \text{and} \quad a_A(\epsilon) = a_R^*(\epsilon). \quad (26)$$

We will see from the final results of this Section that a_R defined by eq. (26) has the meaning of the amplitude of Andreev reflection. In particular, for the ideal BCS superconductors the equilibrium Green's functions are: $g_R(\epsilon) = \epsilon/\delta$, $f_R(\epsilon) = \Delta/\delta$, where $\delta \equiv [(\epsilon + i0)^2 - \Delta^2]^{1/2}$, and eq. (26) reduces to eq. (1) of the previous Section.

After the rotation (25) equation (23) for the retarded Green's function and $p_x > 0$ takes the form

$$iv_F \frac{\partial \tilde{G}_R}{\partial x} = \Omega_R [\sigma_z, \tilde{G}_R], \quad (27)$$

with σ 's here and below denoting Pauli matrices. Combined with eq. (24), this equation means that the matrix structure of the solutions $\tilde{G}_{R1,2}$ decaying in the first and second electrodes respectively, is: $\tilde{G}_{R1,2} \propto \sigma_{\pm}$, so that

$$G_{R1}(\epsilon, \epsilon') = U_R^{-1} \tilde{G}_{R1} U_R = q_1(\epsilon, \epsilon') \begin{pmatrix} a_R(\epsilon') & 1 \\ -a_R(\epsilon) a_R(\epsilon') & -a_R(\epsilon) \end{pmatrix},$$

$$G_{R2}(\epsilon, \epsilon') = U_R^{-1} \tilde{G}_{R2} U_R = q_2(\epsilon, \epsilon') \begin{pmatrix} -a_R(\epsilon) & -a_R(\epsilon) a_R(\epsilon') \\ 1 & a_R(\epsilon') \end{pmatrix},$$

where $q_{1,2}$ are some functions that will be found later.

We discuss in detail the case of a single-mode ballistic constriction with $D = 1$. In this case the total Green's function should be continuous in the constriction:

$$G_{R1}^{(0)} + G_{R1} = G_{R2}^{(0)} + G_{R2}, \quad (28)$$

where $G_{Rj}^{(0)}$ is the equilibrium Green's functions of the j th electrode. Expression (22) for these functions is valid only if the energies ϵ, ϵ' are measured relative to the Fermi energy of the corresponding electrode. If the zero of energy is chosen differently, the energies in eq. (22) should be shifted. For instance, if we chose the zero of energy to coincide with the Fermi level of the first electrode, then

$$G_{R2}^{(0)} = \begin{pmatrix} g_R(\epsilon + u) \delta(\epsilon - \epsilon') & f_R(\epsilon + u) \delta(\epsilon - \epsilon' + 2u) \\ -f_R(\epsilon - u) \delta(\epsilon - \epsilon' - 2u) & -g_R(\epsilon - u) \delta(\epsilon - \epsilon') \end{pmatrix},$$

where $u \equiv eV$, while $G_{R1}^{(0)}$ is still given by eq. (22). Equation (28) represents then the matrix equation that allows us to determine the functions $q_{1,2}$. Indeed, eliminating q_2

from the first row of the matrix equation (28) we obtain the recurrence relation for q_1 :

$$q_1(\epsilon, \epsilon' + 2u) - q_1(\epsilon, \epsilon') a_R(\epsilon') a_R(\epsilon' + u) = (\delta(\epsilon - \epsilon') + g_R(\epsilon)) a_R(\epsilon + u) - f_R(\epsilon + u) a_R(\epsilon') \delta(\epsilon - \epsilon' + 2u). \quad (29)$$

Since the source terms in this relation are δ -functions we can look for a solution in the form $q_1 = \sum_n A_n(\epsilon) \delta(\epsilon - \epsilon' + 2un)$. The recurrence relation for the coefficients A_n that follows from eq. (29), complemented with the condition that A_n should decay at $n \rightarrow \pm\infty$, can be solved directly. We obtain then the total Green's function in the constriction for $p_x > 0$:

$$G_R = \begin{pmatrix} 1 & 0 \\ -2a_R(\epsilon) & -1 \end{pmatrix} \delta(\epsilon - \epsilon') + 2 \sum_{n=1}^{\infty} \delta(\epsilon - \epsilon' + 2un) \prod_{j=1}^{2n-1} a_R(\epsilon + ju) \begin{pmatrix} a_R(\epsilon') & 1 \\ -a_R(\epsilon) a_R(\epsilon') & -a_R(\epsilon) \end{pmatrix}. \quad (30)$$

In the same way we can find the Green's functions for backward propagation ($p_x < 0$):

$$G_R = \begin{pmatrix} 1 & 2a_R(\epsilon) \\ 0 & -1 \end{pmatrix} \delta(\epsilon - \epsilon') + 2 \sum_{n=1}^{\infty} \delta(\epsilon - \epsilon' - 2un) \prod_{j=1}^{2n-1} a_R(\epsilon - ju) \begin{pmatrix} a_R(\epsilon) & a_R(\epsilon) a_R(\epsilon') \\ -1 & -a_R(\epsilon') \end{pmatrix}, \quad (31)$$

and also show explicitly that the advanced functions G_A are related to G_R as follows:

$$G_A(\epsilon, \epsilon', \text{sign}(p_x)) = -G_R^*(\epsilon, \epsilon', -\text{sign}(p_x)). \quad (32)$$

The current in the constriction depends not only on the density of states but also on the occupation of these states. The information about occupation probabilities is contained in the Keldysh Green's function $G_K(\epsilon, \epsilon')$ which satisfy the following equation [41,19]:

$$i \text{sign}(p_x) v_F \frac{\partial G_K}{\partial x} = H_R G_K + H_K G_A - G_R H_K - G_K H_A, \quad (33)$$

where $H_{R,A}$ are the same matrices which determine the evolution of $G_{R,A}$ in eq. (23), $H_K = H_R n - n H_A$, and n is the equilibrium quasiparticle distribution, $n(\epsilon, \epsilon') = \tanh(\epsilon/2T) \delta(\epsilon - \epsilon')$.

Equation (23) implies that solution of eq. (33) can be written as

$$G_K = G_R n - n G_A + G_H, \quad (34)$$

where G_H satisfies the homogeneous equation:

$$i\text{sign}(p_x)v_F\frac{\partial G_H}{\partial x} = H_R G_H - G_H H_A. \quad (35)$$

Calculation of G_H follows closely the one for $G_{R,A}$ that was described above. Diagonalizing $H_{R,A}$ in eq. (35) by transformation (25) and imposing the condition that G_H decays inside the electrodes, we see that for $p_x > 0$ and $x = 0$, $\tilde{G}_{H1,2} \propto (1 \mp \sigma_z)$ in the first and second electrode respectively. From this we find that

$$\begin{aligned} G_{H1}(\varepsilon, \varepsilon') &= U_R^{-1} \tilde{G}_{H1} U_A = \\ &= h_1(\varepsilon, \varepsilon') \begin{pmatrix} 1 & a_A(\varepsilon') \\ -a_R(\varepsilon) & -a_R(\varepsilon)a_A(\varepsilon') \end{pmatrix}, \end{aligned} \quad (36)$$

$$\begin{aligned} G_{H2}(\varepsilon, \varepsilon') &= U_R^{-1} \tilde{G}_{H2} U_A = \\ &= h_2(\varepsilon, \varepsilon') \begin{pmatrix} -a_R(\varepsilon)a_A(\varepsilon') & -a_R(\varepsilon) \\ 1 & a_A(\varepsilon') \end{pmatrix}. \end{aligned} \quad (37)$$

Next we impose the continuity condition $G_{K1} = G_{K2}$ in the constriction, and eliminating h_2 from this condition obtain the recurrence relation for h_1 . This recurrence relation can be solved similarly to the recurrence relation (29) and gives:

$$\begin{aligned} h_1(\varepsilon, \varepsilon') &= 2 \sum_{m=0}^{\infty} \left[\sum_{n=0}^{\infty} \delta(\varepsilon - \varepsilon' + 2un) \prod_{j=1}^{2n+m} a_R(\varepsilon + ju) \right. \\ &\quad \left. \prod_{j=1}^m a_A(\varepsilon' + ju) n^{(-)}(\varepsilon' + mu) + \sum_{n=1}^{\infty} \delta(\varepsilon - \varepsilon' - 2un) \right. \\ &\quad \left. \prod_{j=1}^m a_R(\varepsilon + ju) \prod_{j=1}^{2n+m} a_A(\varepsilon' + ju) n^{(-)}(\varepsilon + mu) \right], \end{aligned} \quad (38)$$

where $n^{(-)}(\varepsilon) \equiv n(\varepsilon + u) - n(\varepsilon)$, and we used the convention that $\prod_{j=1}^0(\dots) = 1$. Equations (36), (38) and (34) determine the Keldysh Green's function in the constriction for $p_x > 0$. Following the same steps we can also find G_K for $p_x < 0$.

The time-dependent current $I(t)$ in the constriction can be expressed in terms of G_K as

$$\begin{aligned} I(t) &= \frac{e}{8\pi\hbar} \int d\varepsilon d\varepsilon' \text{Tr} \left[\sigma_z \left(G_K^{(p_x > 0)}(\varepsilon, \varepsilon') - \right. \right. \\ &\quad \left. \left. - G_K^{(p_x < 0)}(\varepsilon, \varepsilon') \right) \right] \exp^{i(\varepsilon - \varepsilon')t/\hbar}. \end{aligned} \quad (39)$$

For G_K found above (and given by the eqs. (34), (36), (38), (30) and (32)), eq. (39) shows that the current is a combination of harmonics of the Josephson frequency

$\omega_J = 2eV/\hbar$, and the amplitude of the k th harmonics is [25]:

$$\begin{aligned} I_k &= \frac{e}{\pi\hbar} \left[eV \delta_{k0} - \int d\varepsilon \tanh\left(\frac{\varepsilon}{2T}\right) (1 - |a_R(\varepsilon)|^2) \right. \\ &\quad \left. \sum_{m=0}^{\infty} \prod_{j=1}^m |a_R(\varepsilon + jeV)|^2 \prod_{j=m+1}^{m+2k} a_R(\varepsilon + jeV) \right]. \end{aligned} \quad (40)$$

Transformations bringing expression for the current into this form used the relation $a_R(-\varepsilon) = -a_R^*(\varepsilon)$. This relation holds due to assumed electron-hole symmetry of the superconducting electrodes of the constriction.

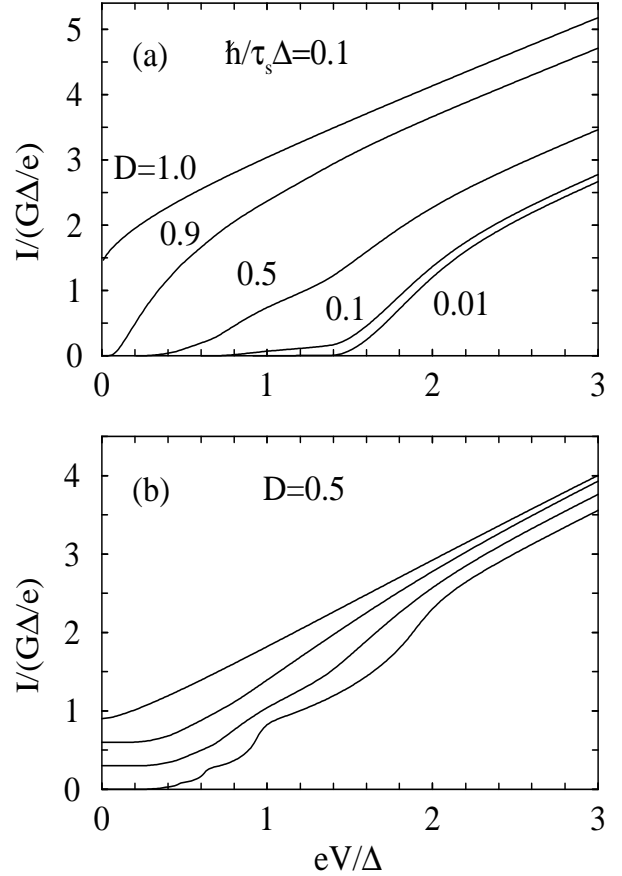


FIG. 3. DC IV characteristics of a single-mode constriction between two superconductors with paramagnetic impurities for several values of (a) constriction transparency D , and (b) spin-flip scattering rate $1/\tau_s$ in the superconductors. G in normalization of the current is the normal-state conductance of the constriction $G = e^2 D/\pi\hbar$. The curves in (b) are shifted for clarity and correspond to (from bottom to top) $\hbar/\tau_s \Delta = 0.01, 0.1, 0.3, 1.0$. For discussion see text.

Comparison of eq. (40) for the Fourier harmonics of the current in a single-mode constriction with the $D = 1$ version of eq. (13) obtained from the BdG equations shows that these two equations coincide if we identify a_R with

the amplitude of the Andreev reflection. To see this equivalence we note that at $D = 1$ the recurrence relations (14) and (15) give that $B_n \equiv 0$ for all n , $A_n = 0$ for $n \leq 0$, and $A_n = \prod_{j=1}^{2n-1} a_j$ for $n > 0$. With these wavefunction amplitudes eq. (13) indeed reduces to eq. (40). This means that the only role of the complex internal structure of the superconducting electrodes (including possible inelastic processes) in determining the ac Josephson current in a short ballistic constriction is to modify the amplitude of the Andreev reflection which is in general given by eq. (26). Starting from the Zaitsev's solution of the constriction problem in the matrix form [20], one can show [42] that this conclusion is valid for arbitrary D . The Fourier components of the time-dependent current in the constriction are determined by eq. (13) and recurrence relations (14) and (15) for general microscopic structure of the superconducting electrodes, if the amplitude of Andreev reflection a_R is defined by eq. (26) [43].

To illustrate this approach, we calculated the IV characteristic of a short constriction between two superconductors with paramagnetic impurities. In this case, the BCS singularity in the density of states at the gap edge is broadened by the spin-flip scattering and the magnitude of the gap itself is suppressed. These two effects are reflected in the energy dependence of the Andreev reflection amplitude $a_R(\varepsilon)$ which can be written in a form similar to eq. (1):

$$a_R(\varepsilon) = u(\varepsilon) - (u(\varepsilon)^2 - 1)^{1/2}, \quad (41)$$

where $u(\varepsilon)$ is given by the equation [44]:

$$\frac{\varepsilon}{\Delta} = u \left(1 - \frac{\hbar/\tau_s \Delta}{(1 - u^2)^{1/2}} \right). \quad (42)$$

Here $1/\tau_s$ is the rate of the spin-flip scattering and Δ is the energy gap in absence of this scattering. Equations (41) and (42) allow for a simple numerical determination of $a_R(\varepsilon)$. DC IV characteristics for zero temperature and several scattering rates $1/\tau_s$ and transparencies D calculated with the $a_R(\varepsilon)$ from eqs. (41) and (42) are plotted in Fig. 3. Figure 3a shows how the IV characteristic evolves as a function of the constriction transparency D at weak spin-flip scattering. We see that even weak scattering results in effective broadening of all current singularities. Due to suppression of the energy gap in the electrodes, the spin-flip scattering also gives rise to suppression of the zero-bias current jump at $D = 1$ and suppression of the excess current. Such a gap suppression becomes progressively more pronounced at larger scattering rates (Fig. 3b), until the gap disappears completely at $\hbar/\tau_s = \Delta$. In the gapless regime, the IV characteristic is practically linear.

IV. NOISE

The method developed in the previous Section allows us to calculate not only the average current in the constriction, but also fluctuations of the current around the average. The spectral density of the current fluctuations $S_I(\omega)$ in presence of the time-dependent average current is defined as

$$S_I(\omega) = \frac{1}{2\pi} \int d\tau e^{i\omega\tau} \overline{K_I(t, t + \tau)}, \quad (43)$$

$$K_I(t, t + \tau) \equiv \frac{1}{2} \langle I(t)I(t + \tau) + I(t + \tau)I(t) \rangle - \langle I(t) \rangle \langle I(t + \tau) \rangle,$$

where the bar over $K_I(t, t + \tau)$ denotes averaging over the time t . In this Section we discuss only the single-mode ballistic constriction. For such a constriction, the correlation function K_I can be expressed in terms of the quasiclassical Green's functions [45]:

$$K_I(t, t + \tau) = -\frac{e^2}{8} \sum_{\pm} \text{Tr} [G_{\pm}^{>}(t, t + \tau) \sigma_z G_{\pm}^{<}(t + \tau, t) \sigma_z + G_{\pm}^{<}(t, t + \tau) \sigma_z G_{\pm}^{>}(t + \tau, t) \sigma_z],$$

where \sum_{\pm} is the sum over the two directions of propagation in the constriction. The Green's functions $G^{>,<}$ are related to the functions $G_{R,A,K}$ discussed in the previous section:

$$G^{>,<} = \frac{1}{2} [G_K \pm (G_R - G_A)]. \quad (44)$$

The functions $G(\varepsilon, \varepsilon')$ are the Fourier transforms of the $G(t, t')$.

If we use in eq. (44) the Green's functions found in the previous section, we see that $G^{>,<}$ can be written as

$$G_{\pm}^{>,<}(\varepsilon, \varepsilon') = \sum_n G_{n,\pm}^{>,<}(\varepsilon + neV) \delta(\varepsilon - \varepsilon' + 2neV), \quad (45)$$

and the spectral density (43) assumes the form:

$$S_I(\omega) = -\frac{e^2}{32\pi^2\hbar} \sum_{n,\pm,\pm\omega} \int d\varepsilon \text{Tr} [G_{n,\pm}^{>}(\varepsilon) \sigma_z G_{-n,\pm}^{<}(\varepsilon \pm \hbar\omega) \sigma_z]. \quad (46)$$

Combining this equation with the equations for the Green's function $G^{>,<}$ (eqs. (44) and (45) of this Section and eqs. (34), (36), (38), (30) and (32) of the previous Section) we arrive at the final result for $S_I(\omega)$ [26]:

$$S_I(\omega) = \frac{e^2}{2\pi^2\hbar} \sum_{\pm\omega} \int d\varepsilon F(\varepsilon) (1 - F(\varepsilon \pm \hbar\omega))$$

$$[1 + 2\text{Re} \sum_{k=1}^{\infty} \prod_{j=1}^k a_R(\varepsilon + jeV) a_A(\varepsilon + jeV \pm \hbar\omega)]. \quad (47)$$

Function F here has the meaning of non-equilibrium distribution of quasiparticles in the constriction:

$$F(\varepsilon) = f(\varepsilon) + \sum_{n=0}^{\infty} \prod_{m=0}^n |a_R(\varepsilon - meV)|^2 [f(\varepsilon - (n+1)eV) - f(\varepsilon - neV)], \quad (48)$$

where $f(\varepsilon)$ is the Fermi distribution function.

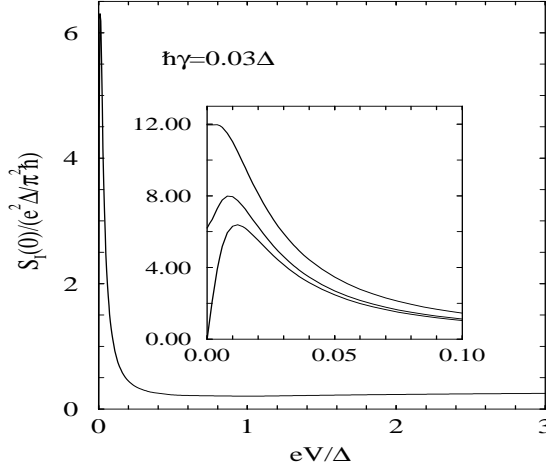


FIG. 4. Zero-frequency spectral density of fluctuations of the current in a single-mode ballistic constrictions at zero temperature as a function of the bias voltage. The peak at low voltages is due to multiple Andreev reflections. The inset shows a blowup of the peak at several temperatures: (from bottom to top) $T/\Delta = 0, 1, 2$.

The spectral density of current fluctuations defined by eqs. (47) and (48) depends strongly on the behavior of the Andreev reflection amplitude $a_R(\varepsilon)$ as a function of energy ε . Figure 4 shows the zero-frequency spectral density $S_I(0)$ calculated numerically for the superconductors with small quasiparticle inelastic scattering rate γ , when $a_R(\varepsilon)$ is given by eq. (41) with

$$u(\varepsilon) = \frac{\varepsilon + i\hbar\gamma/2}{\Delta}.$$

One can see from Fig. 4 that in this case the main feature of the current noise is the peak of $S_I(0)$ at low voltages. The height of the peak is much larger than the classical shot noise result $eI/2\pi$ which in our case would be on the order of $e^2\Delta/2\pi^2\hbar$. To understand the origin of this large noise we evaluate eqs. (47) and (48) analytically in the limit $V \ll \Delta/e$. Expanding the amplitude $a_R(\varepsilon)$ of Andreev reflection in small relaxation rate γ and replacing the sums with the integrals we obtain the spectral density of current fluctuations at low frequencies, $\omega \ll \Delta/\hbar$:

$$S_I(\omega) = \frac{e}{\pi^2\hbar V} \sum_{\pm\omega} \int_{-\Delta}^{\Delta} d\varepsilon F(\varepsilon)(1 - F(\varepsilon \pm \hbar\omega)) \int_{\varepsilon}^{\Delta} d\varepsilon' \exp\left\{-\int_{\varepsilon}^{\varepsilon'} \frac{d\nu\hbar\gamma(\nu)}{eV\sqrt{\Delta^2 - \nu^2}}\right\} \cos\left(\frac{\hbar\omega}{eV} [\arccos(\frac{\varepsilon'}{\Delta}) - \arccos(\frac{\varepsilon}{\Delta})]\right), \quad (49)$$

where the quasiparticle distribution function reduces to

$$F(\varepsilon) = f(\varepsilon) - \int_{-\Delta}^{\varepsilon} d\varepsilon' \frac{\partial f}{\partial \varepsilon'} \exp\left\{-\int_{\varepsilon'}^{\varepsilon} \frac{d\nu\hbar\gamma(\nu)}{eV\sqrt{\Delta^2 - \nu^2}}\right\}. \quad (50)$$

For ideal BCS superconductors $\gamma \rightarrow 0$ and eq. (50) immediately gives that $F(\varepsilon) = f(\Delta)$. Then the spectral density (49) can be found explicitly:

$$S_I(\omega) = \frac{e\Delta^2}{2\pi^2\hbar \cosh^2(\Delta/2T)V} \frac{1 + \cos(\pi\hbar\omega/eV)}{(1 - (\hbar\omega/eV)^2)^2}. \quad (51)$$

This equation shows that the noise diverges at $V \rightarrow 0$ as $1/V$. At finite relaxation rate γ this divergence saturates at $V \simeq \hbar\gamma/e$ and gives the low-voltage peak in Fig. 4. The origin of this unusual voltage dependence of the noise is the process of multiple Andreev reflections. Each quasiparticle entering the constriction with the energy equal to one of the gap edges generates an avalanche of Andreev reflections before it can escape out of the constriction by climbing up or down in energy to the opposite edge of the energy gap. The number of generated Andreev reflections is $2\Delta/eV$, so that each quasiparticle causes a coherent transfer through the constriction of a charge quantum of magnitude $2\Delta/V$. For small voltages $V \ll \Delta/e$ this charge is much larger than the charge of an individual Cooper pair. In this way the randomness of the quasiparticle scattering (quasiparticles get inside the energy gap with probability $f(-\Delta)$ from one electrode and with probability $f(\Delta)$ from the opposite electrode) is amplified. Therefore, the noise described by eq. (51) can be interpreted as the shot noise of these large charge quanta, and we see that the process of multiple Andreev reflections dominates the current noise as well as the average current in short ballistic superconducting constrictions.

This energy-domain picture with cycles of multiple Andreev reflections, together with quantitative eqs. (49) and (50), has the “dual” time-domain formulation in terms of evolution of occupation probabilities of the two quasi-stationary Andreev-bound states localized in the constriction that carry dc Josephson current [46]. An advantage of the time-domain formulation is that it can be generalized in a straightforward way to situations with the time-dependent bias voltage. It is also convenient

in establishing explicit relation between the ac, finite-voltage regime and dc regime in dynamics of superconducting constrictions. In particular it shows how the finite-voltage current noise discussed in this Section goes over into large equilibrium supercurrent noise at vanishing bias voltage [26,47].

V. CONCLUSIONS AND UNSOLVED PROBLEMS

We have seen in the preceeding Sections that all electron transport properties of short superconducting constrictions are determined by the interplay of quasiparticle scattering inside the constriction and Andreev reflection at the interfaces between the constriction and superconducting electrodes. Quantitatively, the scattering process at finite bias voltages across the constriction is described by a set of recurrence relations for the amplitudes of quasiparticle wave functions at energies ε_n shifted by integer number n of quanta of the Josephson oscillation, $\varepsilon_n = \varepsilon + 2eVn$, $n = 0, \pm 1, \dots$. The recurrence relations are valid for general scattering properties of the constriction that are characterized by the set of transmission eigenvalues D_m , and general microscopic structure of the superconducting electrodes characterized by the energy dependence of the Andreev reflection amplitude $a(\varepsilon)$.

In this Chapter, we discussed the constrictions between identical s -wave superconductors. The recurrence relations derived for this situation can be generalized to the case of two different superconductors (see the Chapter by P. Bagwell *et al.* in this volume) and d -wave superconductors [48,49]. An interesting possible direction for generalization of the recurrence relations is the case of transmission coefficient $D(\varepsilon)$ that is energy-dependent on the scale of superconducting energy gap Δ . Such a generalization would allow, for example, a systematic study of the ac Josephson effect through a resonant level [50,51] or thick tunnel barrier. Another important unsolved problem is the extension of the recurrence relations approach to the constrictions with the spin-dependent scattering, for example, Josephson junctions with ferromagnetic interlayer – see the contribution of G. Arnold *et al.* to this volume.

The basic simplification which allows to describe quantitatively such a variety of different situations is the approximation of short constriction $d \ll \xi$. A very important open problem is the lifting of this restriction. General solution of this problem for junctions with $d \simeq \xi$ appears very difficult due to the necessity of self-consistent determination of the distribution of the pair potential $\Delta(x)$ and electrostatic potential $\varphi(x)$. As a first step towards such a solution, it would be interesting to apply the MAR approach to the opposite limit of long junctions $d \gg \xi$. Long disordered SNS junctions have been attracting a lot of attention recently – see, e.g., [52–54] and refer-

ences therein, but the interest has been focused mainly on their properties close to equilibrium. MAR approach can be advantageous in studying strongly non-equilibrium situations. Another challenging unsolved problem is application of the results presented in this chapter to the description of Coulomb blockade in Josephson junctions with large transparency. The Coulomb blockade regime is characterized by quantum dynamics of the Josephson phase difference φ [55,56], in contrast to the classical dynamics of φ assumed in this Chapter.

In summary, one can expect further exciting new developments and rapid progress in understanding of high-transparency Josephson junctions.

-
- [1] T.M. Klapwijk, G.E. Blonder, and M. Tinkham, *Physica B* **109&110** (1982), 1657.
 - [2] A.W. Kleinsasser, R.E. Miller, W.H. Mallison, G.B. Arnold, *Phys. Rev. Lett.* **72** (1994), 1738.
 - [3] H. Takayanagi, T. Akazaki, and J. Nitta, *Phys. Rev. Lett.* **75** (1995), 3533.
 - [4] L.C. Mur, C.J.P.M. Harmans, J.E. Mooij, J.F. Carlin, A. Rudra, and M. Ilegems, *Phys. Rev. B* **54** (1996), R2327.
 - [5] N. van der Post, E.T. Peters, I.K. Yanson, and J.M. van Ruitenbeek, *Phys. Rev. Lett.* **73** (1994), 2611.
 - [6] M.C. Koops, G.V. van Duynveldt, and R. de Bruyn Ouboter, *Phys. Rev. Lett.* **77** (1996), 2542.
 - [7] E. Scheer, P. Joyez, D. Esteve, C. Urbina, and M.H. Devoret, *Phys. Rev. Lett.* **78** (1997), 3535.
 - [8] A. Frydman and Z. Ovadyahu, *Solid State Commun.* **95** (1995), 79.
 - [9] J. Kutchinsky, R. Taboryski, T. Clausen, C.B. Sorensen, A. Kristensen, P.E. Lindelof, J.B. Hansen, C.S. Jacobsen, and J.L. Skov, *Phys. Rev. Lett.* **78** (1997), 931.
 - [10] T. Matsui and H. Ohta, *IEEE Trans. Appl. Appl. Supercond.* **5** (1995), 3300.
 - [11] B.N. Taylor and E. Burstein, *Phys. Rev. Lett.* **10** (1963), 14.
 - [12] C.J. Adkins, *Rev. Mod. Phys.* **36** (1964), 211.
 - [13] I.K. Yanson, V.M. Svistunov, and I.M. Dmitrenko, *Sov. Phys. - JETP* **20** (1965), 1404.
 - [14] S.M. Markus, *Phys. Lett.* **19** (1966), 623; **20** (1966), 236.
 - [15] J.M. Rowell and W.L. Feldman, *Phys. Rev.* **172** (1968), 393.
 - [16] L.J. Barnes, *Phys. Rev.* **184** (1969), 434.
 - [17] A.A. Bright and J.R. Merrill, *Phys. Rev.* **184** (1969), 446.
 - [18] J.R. Schrieffer and J.W. Wilkins, *Phys. Rev. Lett.* **10** (1963), 17.
 - [19] A.V. Zaitzev, *Sov. Phys. - JETP* **51** (1980), 111.
 - [20] A.V. Zaitzev, *Sov. Phys. - JETP* **59** (1983), 1015.
 - [21] G.B. Arnold, *J. Low Temp. Phys.* **59** (1985), 143; **68** (1987), 1.
 - [22] E.N. Bratus, V.S. Shumeiko, and G. Wendin, *Phys. Rev. Lett.* **74** (1995), 2110.

- [23] D.V. Averin and A. Bardas, Phys. Rev. Lett. **75** (1995), 1831.
- [24] U. Günsenheimer and A.D. Zaikin, Phys. Rev. B **50** (1994), 6317.
- [25] D.V. Averin and A. Bardas, Phys. Rev. B **53** (1996), R1705.
- [26] D.V. Averin and H.T. Imam, Phys. Rev. Lett. **76** (1996), 3814.
- [27] I.O. Kulik and A.N. Omel'yanchuk, Sov. J. Low Temp. Phys. **3** (1977), 459.
- [28] A. Bardas and D.V. Averin, cond-mat/9706087.
- [29] A. Furusaki and M. Tsukada, Sol. State Commun. **78** (1991), 299.
- [30] C.W.J. Beenakker, Phys. Rev. Lett. **67** (1991), 3836.
- [31] S. Datta, P.F. Bagwell, M.P. Antram, Phys. Low-Dim. Struct. **3** (1996), 1.
- [32] Yu.V. Nazarov, in: *Quantum Dynamics of Submicron Structures* (Kluwer, Amsterdam, 1995), p. 687.
- [33] C.W.J. Beenakker and M. Büttiker, Phys. Rev. B **46** (1992), 1889.
- [34] K.E. Nagaev, Phys. Lett. A **169** (1992), 103.
- [35] E.N. Bratus, V.S. Shumeiko, and E.V. Bezuglyi, J. Low Temp. Phys. **22** (1996), 474.
- [36] S.N. Artemenko, A.F. Volkov, and A.V. Zaitsev, Sov. Phys. - JETP **49** (1979), 924.
- [37] I.O. Kulik and A.N. Omel'yanchuk, JETP Lett. **21** (1975), 96.
- [38] L.G. Aslamazov and A.I. Larkin Sov. Phys. - JETP **43** (1976), 698.
- [39] C. Nguyen, H. Kroemer, and E.L. Hu, Phys. Rev. Lett. **69** (1992), 2847.
- [40] J. Rammer and H. Smith, Rev. Mod. Phys. **58**, 323 (1986).
- [41] A.I. Larkin and Yu.N. Ovchinnikov, Sov. Phys. - JETP **41**, 960 (1976).
- [42] A.V. Zaitsev and D.V. Averin, cond-mat/9708190.
- [43] A similar recurrence relation can be obtain within the approach based on the tight-binding Hamiltonian, see J. C. Cuevas, A. Martín-Rodero, and A. Levy Yeyati, Phys. Rev. B **54** (1996), 7366.
- [44] K. Maki, in: *"Superconductivity"*, ed. by R.D. Parks, (Marcel Dekker, NY, 1969), p. 1035.
- [45] V.A. Khlus, Sov. Phys. - JETP **66**, 1243 (1987).
- [46] D.V. Averin, Physica B **227** (1996), 241.
- [47] A. Martín-Rodero, A. Levy Yeyati, and F.J. García-Vidal, Phys. Rev. B **53** (1996), R8891.
- [48] Y. Tanaka and S. Kashiwaya, Phys. Rev. B **53** (1996), R11957.
- [49] M. Hurd, cond-mat/9702028.
- [50] A. Levy Yeyati, J. C. Cuevas, A. Lopez-Davalos, A. Martín-Rodero, Phys. Rev. B **55** (1997), R6137.
- [51] G. Johansson, V.S. Shumeiko, E.N. Bratus, and G. Wendin, Physica C, to be published.
- [52] A.V. Zaitsev, JETP Lett. **61** (1995), 771.
- [53] A.F. Volkov and H. Takayanagi, Phys. Rev. Lett. **69** (1996), 4026.
- [54] F. Zhou and B. Spivak, Pis'ma v ZhETF **65** (1997), 347.
- [55] D.V. Averin and K.K. Likharev, in: *Mesoscopic Phenomena in Solids*, ed. by B.L. Altshuler, P.A. Lee, and R.A. Webb, (Elsevier, Amsterdam, 1991), p. 173.
- [56] G. Schön and A.D. Zaikin, Phys. Rep. **198** (1990), 237.